

Influence of the resonant interaction of surface magnetostatic waves with exchange modes on the EMF generation in YIG/Pt structures

© M.E. Seleznev,^{1,2} Yu.V. Nikulin,^{1,2} V.K. Sakharov,¹ Yu.V. Khivintsev,^{1,2} A.V. Kozhevnikov,¹ S.L. Vysotskiy,^{1,2} Yu.A. Filimonov^{1,2}

¹ Saratov Branch, Kotelnikov Institute of Radio Engineering and Electronics, Russian Academy of Sciences, 410019 Saratov, Russia

² Saratov National Research State University, 410012 Saratov, Russia
e-mail: mixanich94@mail.ru

Received April 30, 2021

Revised April 30, 2021

Accepted April 30, 2021

The characteristics of EMF (U) generation in the thin-film Pt/YIG structures caused by hybridization of propagating magnetostatic surface waves with exchange modes of YIG film were studied. It was shown that at frequencies f^* corresponding to the dipole-exchange resonances (DER) the magnitude of EMF U increases by several times in comparison with the frequencies different from DER ($f \neq f^*$). The Volt-Watt sensitivity was estimated for the Pt/YIG structures with different geometries of Pt microstrips.

Keywords: Spintronics, spin waves, EMF generation, electron drag effect, dipole-exchange resonance.

DOI: 10.21883/TP.2022.13.52224.136-21

Introduction

Study of spin waves propagation and EMF generation in magnetic dielectric-metal structures is of interest for creation of energy-efficient element base on the principles of magnonics and spintronics [1-3]. One of the tasks of these areas is the studying the mechanisms and improvement of efficiency of spin waves conversion to electric current at ferrite-conductor interface and within conductor volume. Therefore, the structures, based on yttrium iron garnet (YIG) and platinum (Pt) — metal with a strong spin-orbit coupling, are studied the most. In such structures the metal conduction electrons are sensitive to magnetization of YIG film due to exchange and spin-orbital interaction, resulting in EMF generation at spin wave propagation by means of Hall spin effect [4] or wave drag effect in conductor volume [5-7]. But there were no studies of dipole-exchange resonances influence on the generated EMF at SMSW propagation in Pt/YIG structures yet.

In this work we studied the specifics of EMF (U) generation in the thin-film Pt/YIG structures for the case, when in YIG film the propagating surface magnetostatic waves (SMSW) are hybridized with exchange volume modes of YIG film.

1. Structure study and experimental technique

For the structures making the YIG film with thickness of $d \sim 900$ nm with effective saturation magnetization of $4\pi M^{\text{eff}} \sim 1800$ G and ferromagnetic resonance linewidth of $2\Delta H \sim 0.6$ Oe, grown on gadolinium-gallium garnet

(GGG) substrate was used (YIG film is marked with number 5, Fig. 1). Pt film with thickness of $t \sim 9$ nm was grown on surface of YIG film, using magnetron sputtering method, and from this Pt film the structures of three types were formed using photolithography and ion-beam etching methods (1-3, Fig. 1). Structure 1 (Fig. 1, a) on YIG surface had a single Pt microstrip with length of $L \sim 220 \mu\text{m}$ and width of $W \sim 200 \mu\text{m}$ and specific resistivity of $\rho \sim 0.41 \cdot 10^{-6} \Omega \cdot \text{m}$ ($R_{\square} \sim 0.41 \cdot 10^2 \Omega/\mu\text{m}$). In structure 2 (Fig. 1, b) on YIG film surface a single Pt microstrip with width of $W \sim 40 \mu\text{m}$, $L \sim 220 \mu\text{m}$ and $\rho \sim 0.324 \cdot 10^{-6} \Omega \cdot \text{m}$ ($R_{\square} \sim 0.41 \cdot 10^2 \Omega/\mu\text{m}$) was formed. Structure 3 (Fig. 1, c) contained three Pt microstrips, connected in series with a copper conductor, with $L \sim 220 \mu\text{m}$, $W \sim 40 \mu\text{m}$ and $\rho \sim 0.32 \cdot 10^{-6} \Omega \cdot \mu\text{m}$ ($R_{\square} \sim 0.32 \cdot 10^2 \Omega/\mu\text{m}$). Pt microstrips were formed between copper microantennas (1 and 2), integrated on YIG film surface and located on a distance of $250 \mu\text{m}$ from each other, with aperture (length) of $a \sim 250 \mu\text{m}$ and width of $b \sim 4 \mu\text{m}$. Copper contacts (3 and 4) were formed for measuring the EMF, generated in the structures, on Pt microstrips ends over the whole width W .

During the studies the structures were located between electric magnet poles in such a way, that magnetic field $H \sim 939$ Oe was directed at a tangent to YIG film surface and perpendicular to a length L of microstrips, corresponding to SMSW excitation geometry. Measurement of frequency dependencies of module and phases of the coefficients of transmission (S_{12}) and reflection (S_{22}) of spin waves was performed using a vector network analyzer, connected to the microantennas (1 and 2), integrated on YIG film surface, using microwave microprobes (Fig. 1).

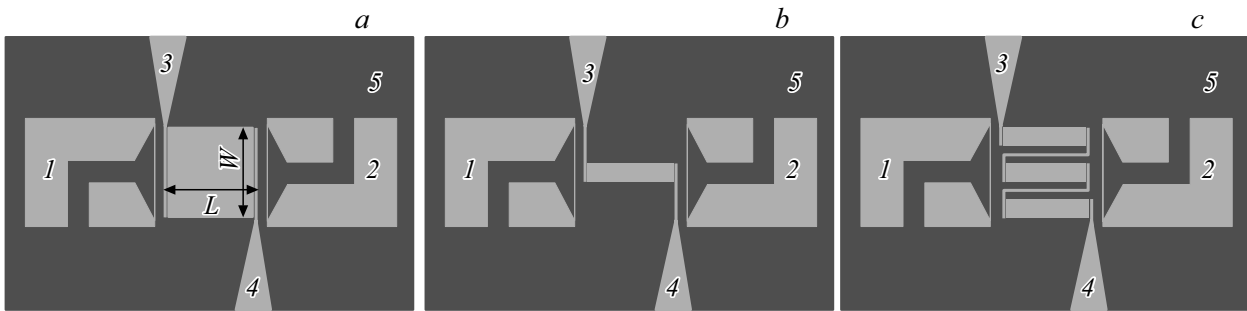


Figure 1. Pt/YIG microstructures as a single Pt microstrip with length of $L \sim 220 \mu\text{m}$ and width of $W \sim 200 \mu\text{m}$ (a); single Pt microstrip with $L \sim 220 \mu\text{m}$ and $W \sim 40 \mu\text{m}$ (b) and three series-connected Pt microstrips with $L \sim 220 \mu\text{m}$ and $W \sim 40 \mu\text{m}$ each (c). 1, 2 — feed microantennas; 3, 4 — copper contacts for measuring the generated voltage; 5 — YIG film surface.

Study of the frequency dependence of EMF $U(f)$, generated at SMSW propagation, was performed using a selective voltmeter, connected to contacts 3 and 4 (Fig. 1). At the same time for voltmeter operation the microwave signal with pulse modulation (11.33 kHz) was sent to input antenna, also contributing to lowering the heating influence on the registered EMF.

2. Results and discussion

Fig. 2, a shows the frequency dependencies of the amplitude of the transmission coefficient $S_{12}(f)$, observed at input power of $P \sim -20 \text{ dBm}$ for structures 1-3 (curves 1-3, respectively) and YIG film (curve 4). The lowest values of S_{12} compared to YIG film were observed for structure 3, that can be explained not only with SMSW absorption by Pt strips, but also with influence of copper contacts to Pt strips on SMSW excitation efficiency and propagation conditions. The highest values of S_{12} were registered for the structure 2, where width W of Pt microstrip and length of copper contact paths to Pt were the lowest among structures 1-3.

Fig. 2, b shows the calculated, similar to [8], based on the observed phase-frequency dependencies $\varphi(f)$, dispersion characteristics $k(f)$, where k is SMSW wave number. In structure 2 the SMSW with the highest values of $k \sim 11000 \text{ cm}^{-1}$, that were close to the measured values of $k \sim 12000 \text{ cm}^{-1}$ for structure without platinum (curves 2 and 4 in Fig. 2, b), were also observed. It should be noted that the built dispersion characteristics $k(f)$ of structures 1-3 in the area of wave numbers of $k \leq 6000 \text{ cm}^{-1}$ were almost the same as during calculation for dipole SMSW of Damon-Eshbach type in unsupported film with the selected parameters (curve 5 in Fig. 2, b). However, for $k > 6000 \text{ cm}^{-1}$ the measurement and calculation results are significantly different. Such behavior of the measured dispersion indicates the non-homogeneity of the film parameters in terms of thickness and can be explained with increase of the film effective magnetization in sub-surface layer.

The presence of frequencies, on which the level S_{12} significantly (by 5–15 dB) drops (see sections of characteristic

$S_{12}(f)$ marked with an asterisk on curve 4 in Fig. 2, a) should be noted. Such features in SMSW transmission spectra reflect the resonance interaction of SMSW with exchange volume modes of a film waveguide and are related to resonant increase of SMSW losses [9]. At the same time, in dispersion dependence $k(f)$ on frequencies of dipole-exchange resonances the abnormal dispersion sections appear [9], as it is shown on the insert of Fig. 2, b for the resonance frequency of $\sim 4.645 \text{ GHz}$.

Fig. 2, c shows the frequency dependencies of the generated EMF $U(f)$ for the studied structures at input excitation power $P_{in} \sim -5 \text{ dBm}$. It can be observed that dependencies of $U(f)$ for all studied structures demonstrate the resonant increase of signal U on frequencies, corresponding to the frequencies of dipole-exchange resonances. To illustrate that, the sections of the dependence $S_{12}(f)$ and $U(f)$, containing resonance features, are presented in Fig. 3, a, b for narrow frequency band. It can also be observed that at frequencies of $f > 5 \text{ GHz}$ the value of the generated EMF significantly drops.

The observed decrease of U at frequencies of $f > 5 \text{ GHz}$ can be related to decrease of the coefficient of conversion $K(f)$ of input power of $P_{in}(f)$ to SMSW power of $P(f) = K(f) \cdot P_{in}(f)$ for SMSW with wavelength of $\lambda < 2 \cdot b$ ($k > \pi/b \sim 8000 \text{ cm}^{-1}$) by antennas. This is confirmed with calculation of dependencies of $K(f)$ for structures 1-3 using equation

$$K(f) = \frac{P(f)}{P_{in}(f)} = 10^{[S_{22}(f,h)/10]} - 10^{[S_{22}(f,H^*)/10]},$$

where $S_{22}(f, H)$ and $S_{22}(f, H^*)$ are coefficients of reflection of incident power from input antenna at fields of $H \sim 939 \text{ Oe}$ and $H^* \sim 2473 \text{ Oe}$, at which the antenna excites and does not excite SMSW at the selected frequency f , respectively. Fig. 3, a shows that values of $K(f)$ significantly drops at frequencies $f > 5 \text{ GHz}$, at which SMSW are characterized with the wave numbers $k > \pi/b \sim 8000 \text{ cm}^{-1}$ (Fig. 2, b).

To understand the mechanism of EMF generation let's examine Fig. 3, c, where the frequency dependencies of the generated EMF $U(f)$ of structure 3 at SMSW propagation

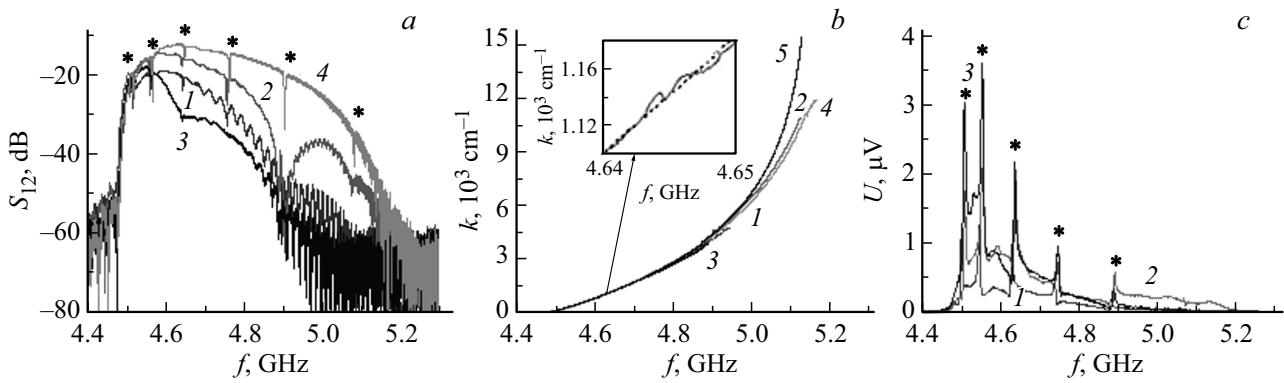


Figure 2. Frequency dependencies of transmission coefficient S_{12} (a), wave number k of SMSW (b) and generated EMF (c) at field $H \sim 939$ Oe. 1-3 — results for structures 1-3, respectively; 4 — results for YIG film; 5 — theoretical calculation of SMSW dispersion. Insert of Fig. 2, b shows the dispersion dependencies near frequency of ~ 4.645 GHz, measured for YIG film (solid line) and calculated for dipole SMSW (dashed line).

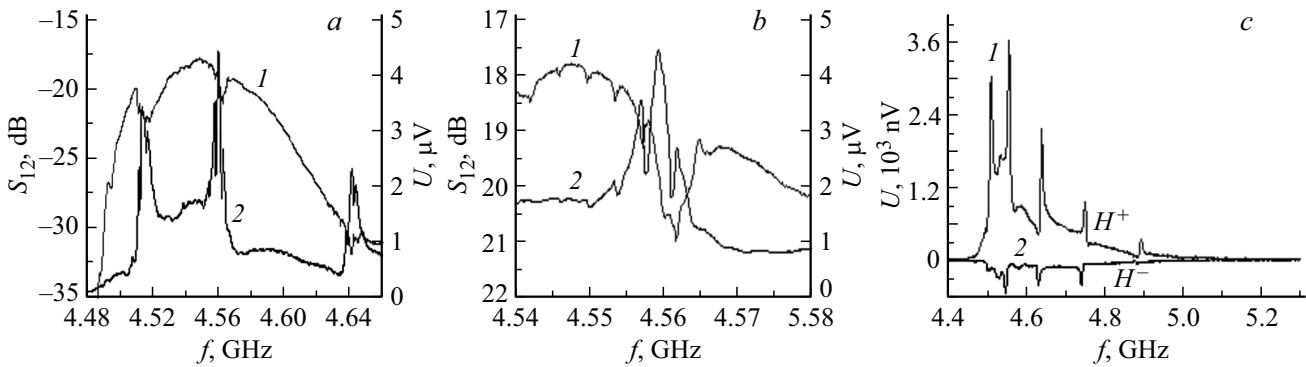


Figure 3. Frequency dependencies of transmission coefficient S_{12} (1) and generated EMF $U(f)$ (2) of structure 3 at frequency range near several dipole-exchange resonances (a) and near single resonance (b); c — frequency dependencies of EMF $U(f)$ at propagation in the same direction of SMSW along the interfaces of Pt/YIG (1) and YIG/GGG (2), that was achieved by a change of direction of superposed magnetization of H^+ to opposite H^- . Magnetic field $H \sim 939$ Oe.

in the same direction, but with SMSW fields localization on interfaces of Pt/YIG and YIG/GGG, are shown. Change of surface, along which SMSW was propagated, was achieved by means of change of direction of the external magnetic field of H^+ to the opposite H^- . At the same time, a change of the sign of the generated EMF $U(f)$ was observed, that can indicate that the main mechanism of EMF generation in Pt/YIG structures is a reverse spin-Hall effect [3], not drag effect or thermal heating of structure [5-7]. Indeed, EMF sign, related to the mentioned effects, should not change at change of the field direction [5]. Thus, the conclusion can be made, that EMF signal increase at frequencies of dipole-exchange resonances can be related to amplification of the spin current at Pt/YIG interface by the exchange modes, propagating over YIG film thickness.

Let's discuss now the Volt-Watt sensitivity $S(f) = U(f)/(P_{in} \cdot K(f))$ and the generated signal $U(f)$ dependence on width and number of platinum microstrips in the examined structures (Fig. 1). With spin pumping mechanism the value of spin current j_s , flowing through Pt/YIG interface, will be defined with linear (as per antenna

length a) power of SMSW $P' = P/a$ and area $S = W \cdot L$ of Pt/YIG contact: $j_s \sim P' \cdot S$. The EMF signal generated due to reverse spin-Hall effect: $U \sim j_s$, $R_{Pt} \sim P' \cdot \rho \cdot L^2/t$, where $R_{Pt} = \rho \cdot L/(W \cdot t)$ is platinum film resistance. At the same time, the generated EMF does not depend on Pt film width, like it was observed earlier for EMF drag in structures of InSb/YIG [10]. As applied to the examined structures 1-3, this should appear in equal values of U for structures 1 and 2 and threefold value of EMF for structure 3.

Fig. 4, b shows the calculated frequency dependencies of the structures sensitivity $S(f) = U(f)/(P_{in} \cdot K(f))$. It can be observed that at frequencies of $f \sim 4.5-4.55$ GHz the sensitivity of structure 3 reached the values of $S \sim 0.023$ V/W, and at frequencies of dipole-exchange resonances — $S \sim 0.06$ V/W, while sensitivity of structure 2 at the same frequencies reached the values of $S \sim 0.011$ and 0.03 V/W, respectively, that is half as much in average. Sensitivity $S(f)$ of structure 1 at almost the whole frequency range was 2-3 times less compared to $S(f)$ of structures 2

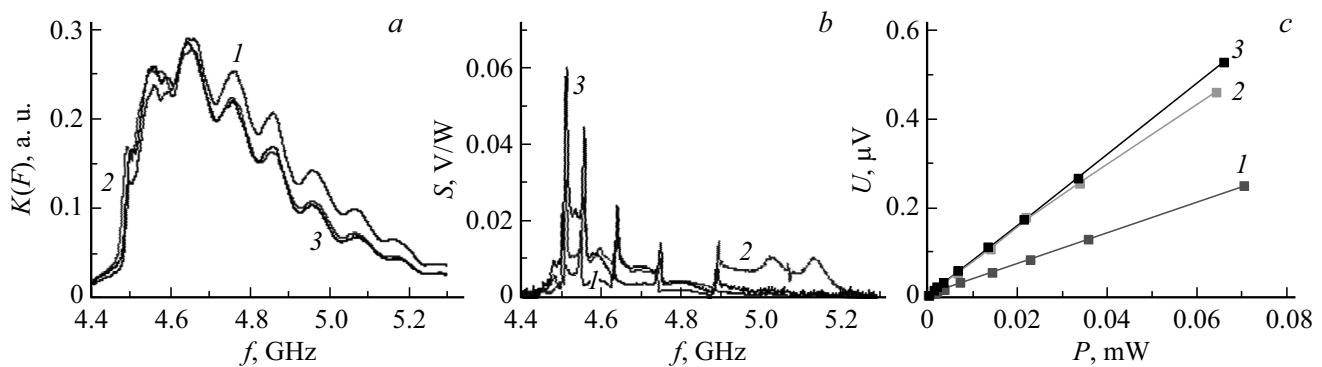


Figure 4. Calculated frequency dependencies of coefficient of conversion $K(f)$ (a) and sensitivity $S(f)$ (b); c — measured dependence of $U(P)$ at frequency of 4.7 GHz and field of $H \sim 939$ Oe. 1-3 — results for structures 1-3, respectively.

and 3. However, at frequencies $f > 4.55$ GHz the similar values of sensitivity of structures 2 and 3 were observed.

Fig. 4, c shows the EMF dependencies at the fixed SMSW excitation frequency of $f = 4.7$ GHz. It can be observed that EMF values for structures 2 and 3 are similar. One of the reasons of $S(f)$ dependencies match for structures 2 and 3 at frequencies of $f > 4.55$ GHz can be the influence of Cu contact path on the nature of SMSW propagation in structure 3 and distribution of linear power P' in the structure plane.

It should be noted that the examined effect of exchange oscillations of EMF in Pt(9nm)/YIG(900nm) structure is essentially different than exchange oscillations of EMF drag in InSb/YIG structure [7]. Indeed, in study [7] EMF in InSb/YIG structures was resonantly decreased at frequencies of dipole-exchange resonances and looked similar to dependencies of $S_{12}(f)$, presented with curve 4 in Fig. 2, a or curves 1 in Fig. 3, a, b. Also, as per electrons drag theory [5,6], the EMF signal $U(f)$ should be increased by the propagating spin waves with k increase. This effect can substantially compensate the $K(f)$ coefficient drop in the short wave end of SMSW spectrum and allow to detect EMF near short wave limit of SMSW spectrum [4-7].

Conclusion

EMF $U(f)$ generation in Pt(9 nm)/YIG(900 nm) structures at SMSW propagation in YIG film under conditions of dipole-exchange resonances forming was studied. It was revealed that at frequencies of the dipole-exchange resonances of SMSW the generated EMF $U(f)$ can increase by several times. At the same time, the Volt-Watt sensitivity at frequencies of the dipole-exchange resonances in the examined case reached the values of $S \sim 0.06$ V/W, that is almost three times higher than in the adjacent frequency areas.

Funding

The study was performed under the Government Task with partial financial support from the Russian Foundation for Basic Research (projects №19-37-90099, 20-07-00968).

Conflict of interest

The authors declare that they have no conflict of interest.

References

- [1] A. Li, W. Zhang, V. Tyberkevych, W.K. Kwok, A. Hoffmann, V. Novosad. *J. Appl. Phys.*, **128** (13), 130902 (2020).
- [2] A. Hirohata, K. Yamada, Y. Nakatani, I.L. Prejbeanu, B. Diény, P. Pirro, B. Hillebrands. *J. Magn. Magn. Mater.*, **509**, 166711 (2020).
- [3] V.E. Demidov, S. Urazhdin, A. Anane, V. Cros, S.O. Demokritov. *J. Appl. Phys.*, **127** (17), 170901 (2020).
- [4] U.V. Nikulin, M.E. Seleznev, Y.V. Khivintsev, V.K. Sakharov, E.S. Pavlov, S.L. Vysotskii, A.V. Kozhevnikov, Y.A. Filimonov. *Semiconductors*, **54**, 1721 (2020).
- [5] Yu.V. Gulyaev, P.E. Zilberman, A.O. Raevsky. *ZhETF*, **76**, (5), 1593 (1979).
- [6] A.S. Bugaev, O.L. Galkin, Yu.V. Gulyaev, P.E. Zilberman. *Pis'ma v ZhTF*, **8**, 485 (1982).
- [7] G.T. Kazakov, A.G. Sukharev, Yu.A. Filimonov, S.K. Nurdzhanova, B.P. Nam, A.S. He. *RE*, **23** (4), 807 (1988).
- [8] Y. Khivintsev, Y. Filimonov, S. Nikitov. *Appl. Phys. Lett.*, **106**, 052407 (2015).
- [9] Yu.V. Gulyaev, A.S. Bugaev, P.E. Zilberman, I.A. Ignatyev, A.G. Konovalov, A.V. Lugovskoy, A.M. Mednikov, B.P. Nam, E.I. Nikolaev. *Pis'ma v ZHETF*, **30**, 600 (1979).
- [10] S.L. Vysotsky, G.T. Kazakov, A.G. Sukharev, Yu.A. Filimonov. *Byull. izobr.* **1** (1988).